A Multiscale Interaction Model for the Origin of the Tropospheric QBO

B. N. GOSWAMI*

Centre for Atmospheric Sciences, Indian Institute of Science, Bangalore, India

(Manuscript received 30 August 1993, in final form 29 July 1994)

ABSTRACT

A conceptual model for the origin of the tropospheric quasi-biennial oscillation (QBO) is presented. It is argued that the tropospheric QBO may not be a fundamental mode of oscillation of the tropical coupled system. It is proposed that it may arise due to multiscale interactions between high-frequency synoptic and intraseasonal oscillations of the atmosphere and a low-frequency oscillation of the coupled system in the presence of the annual cycle. This is demonstrated using a conceptual low-order system consisting of three variables representing the nonlinear atmospheric oscillations and a linear oscillator representing the low-frequency coupled mode. The annual cycle and coupling to the low-frequency linear oscillator provide slowly varying forcings for the atmospheric high-frequency oscillations. The atmospheric oscillations go through a chaotic regime during a certain part of the slowly varying forcing. Such variable forcing introduces a low-frequency tail in the spectrum of the atmospheric high-frequency oscillations. This low-frequency tail resonantly interacts with the low-frequency oscillation and produces the QBO in addition to broadening the spectrum of the low-frequency oscillator. The conceptual model simulates features similar to many observed features of the tropospheric QBO but depends on the assumption that there is an inherent low-frequency El Niño–Southern Oscillation oscillation with a four-year period that occurs independently of the high-frequency forcing or the QBO.

1. Introduction

Tropospheric quasi-biennial oscillation (QBO) has been noted in many early studies (Berlage 1955; Landsberg et al. 1963). More recently, the tropospheric QBO has been documented in many fields (Trenberth 1975, 1976, 1980; Trenberth and Shin 1984; Rasmusson et al. 1981, 1990; Barnett 1983, 1991; van Loon and Shea 1985; Deser and Wallace 1987; Ropelewski and Halpert 1987a,b; Yasunari 1989; Ropelewski et al. 1992). The recent studies have brought out some interesting features of this oscillation. Some of the salient features brought out by these studies are

1) Apart from the annual cycle, the low-frequency variability in the Tropics is dominated by a QBO (with period close to two years) and a low-frequency oscillation (LFO) (with period close to four years). The variance explained by these two oscillations are comparable, with the LFO containing generally more energy than the QBO (Barnett 1991).

2) Both the QBO and the LFO are integral parts of the El Niño and Southern Oscillation (ENSO) cycle and are strongly linked with the mean annual cycle.

3) While the QBO in SST has the largest amplitude in the central and eastern Pacific, the QBO in the surface wind has the largest amplitude in the eastern Indian Ocean and western Pacific.

4) While the LFO appears to be a standing wavenumber-1 oscillation, the QBO shows a definite eastward propagation of energy from southeast Asia (Ropelewski et al. 1992; Barnett 1991).

5) Although some studies (Yasunari 1989) indicate a possible link between stratospheric QBO and tropospheric QBO, the evidence that is available is far from convincing. In fact, other studies (e.g., Barnett 1991) have found no simple relation between classical measures of the stratospheric QBO and the tropospheric QBO. While the stratospheric QBO has no zonal structure, the tropospheric QBO has a clear zonal structure (Rasmusson et al. 1990; Ropelewski et al. 1992).

These recent analyses have put to rest some suspicion (e.g., Landsberg et al. 1963) whether the tropospheric QBO is an artifact of filtering and analysis and have established that it is a clear climatic signal in the Tropics that is strongly linked with ENSO as well as the annual cycle. There have been various physical mechanisms proposed to explain the origin of this biennial variability. Brier (1978) and Nicholls (1978) proposed that air–sea interactions, with annual cycle forcing (solar heating) of opposite polarity associated with winter–summer states, may give rise to a QBO in the Tropics as a subharmonic of the annual cycle through nonlinear

* Current affiliation: Program in Atmospheric and Oceanic Sciences, Princeton University, Princeton, New Jersey.

Corresponding author address: Dr. B. N. Goswami, Program in Atmospheric and Oceanic Sciences, Princeton University, P.O. Box CN710, Sayre Hall, Princeton, NJ 08544-0710.

interactions. Several aspects of these models need improvement and elucidation. First, since the time of the Brier and Nicholls papers, a better understanding of the air–sea interaction processes associated with the low-frequency variability in the Tropics has evolved. Second, the strong and clear association of the QBO with the ENSO cycle, as evidenced by the recent analyses (Rasmusson et al. 1990; Barnett 1991; Ropelewski et al. 1992), was not addressed directly by Brier and Nicholls. More recently, based on the analysis of outgoing longwave radiation, clouds, precipitation, and sea level pressure over the Indian and Pacific sectors, Meehl (1987, 1993) proposed that the QBO may be a modulation of the annual cycle achieved through large-scale air–sea interactions. For example, a year with warm SST in one season leads to greater convection and stronger winds (e.g., strong monsoon; a strong annual cycle), which leads to higher evaporation and colder SST in the following season. If the colder conditions persist till next year, it results in weaker convection and weaker winds (e.g., a weak monsoon; a weak annual cycle). This may lead to lesser evaporation and warmer SST in the following year. The crucial element in this scenario is the persistence of the cold (warm) SST for the next three seasons. Meehl (1993) provides some evidence that the upper-ocean heat content in this region indeed shows similar signatures. Based on calculation of nonlinear interaction coefficients from observations, Barnett (1991) argues that it is unlikely that the QBO is a subharmonic of the annual cycle arising from nonlinear interactions of the annual cycle with itself. It appears that the process described by Meehl (1993) may work intermittently. In this article, we present an alternative conceptual model for the origin of the tropospheric QBO. The conceptual model combines current understanding of the air–sea interactions associated with the large-scale low-frequency variability in the Tropics and the new observational evidences. The additional new element in our model is the role of the higher-frequency oscillations in the atmosphere (synoptic and intraseasonal) in modulating the air–sea interactions. We show that the tropospheric QBO may arise due to a complex interaction between a specified low-frequency ENSO mode, the annual cycle, and the nonlinear atmospheric high-frequency oscillations such as the Madden–Julian oscillations (MJO) and synoptic disturbances. The conceptual model is described in section 2. Section 3 contains results from the simple low-order model and discusses the importance of the different physical processes. Main results are summarized and some concluding remarks are made in section 4.

2. The conceptual model

Any model of the tropospheric QBO must take into account (a) the strong air–sea interactions associated with it, as evidenced by the coherence between atmospheric and oceanic fields, (b) the strong and apparently dominant association with the ENSO, and (c) the clear link with the annual cycle. The spectrum of ENSO indices based on recent data (Rasmusson and Carpenter 1982; Rasmusson et al. 1990) shows a low-frequency peak with a period of 3.7 years. However, this is a broadband spectrum with an interval between recurrences varying around this mean period. Using historical data on ENSO collected by Quinn (1992) between 1525–1988, Diaz and Pulwarty (1992) showed that the mean recurrence interval may have varied significantly in the past. The longest recurrence interval (approximately 12 years) occurred in the 17th century, while the 19th century saw the shortest recurrence interval (approximately 2.5 years). From this long time series it can be seen that the average recurrence period for moderate or stronger El Niño events is close to 4.5 years. Autospectrum of this long time series also shows a significant peak in the interannual timescale with a period of 3.4 years together with some lower-frequency oscillations and the quasi-biennial mode. Thus, the quasi-four-year ENSO signal is a dominant mode of oscillation in the interannual timescale even though the exact period of oscillation may have gone through some changes over the centuries. Many theoretical studies (Hirst 1986; Wakata and Sarachik 1991; Goswami and Selvarajan 1991; Philander et al. 1984; Battisti and Hirst 1989; Neelin 1991) have shown that the tropical coupled ocean–atmosphere system may sustain a low-frequency unstable mode in addition to a few weaker intraseasonal unstable modes. Similarly, simple modeling (Cane and Zebiak 1985; Zebiak and Cane 1987; Anderson and McCreary 1985; Schopf and Suarez 1988; Yamagata and Masumoto 1989), low-resolution-coupled general circulation modeling (Meehl 1990; Sperber and Hameed 1991; Lau et al. 1992; Nagai et al. 1992), and high-resolution coupled modeling (Philander et al. 1992; Latif et al. 1993) studies have shown that the ENSO cycle may be a natural aperiodic oscillation of the tropical coupled ocean–atmosphere system with a dominant period of about four years. The physical mechanism responsible for the dominant four-year periodicity is still a subject of active debate, although a few plausible scenarios have emerged in the last few years. The ENSO cycle may result from a balance between a positive feedback associated with unstable air–sea interactions, as envisioned by Bjerknes (1969), and a negative feedback associated with the Rossby wave reflection from the western boundary. This leads to a delayed oscillation (Suarez and Schopf 1988). In this delayed oscillator scenario, the equatorial wave dynamics play an important role. In another scenario, not the equatorial waves, but a "slow SST mode" (Neelin 1991) may be responsible for the low-frequency (LF) ENSO oscillations seen in global coarse-grid coupled models. The delayed oscillator mechanism and the slow SST mode may arise in a different parameter regime of the tropical

coupled system (Neelin 1991; Latif et al. 1993). Thus, they are probably not independent scenarios. In any case, we note that these proposed physical processes leading to the LF oscillation have all emerged mainly from simple coupled models. The observed coupled system, as well as the more detailed coupled GCMs, seem to have interannual variability that is much more complicated. While there exists these uncertainties about the physical mechanism responsible for the ENSO, it is undoubtedly the dominant LF oscillation in the Tropics in the interannual timescale. From the broadband nature of the spectrum, however, it is clear that in addition to this dominant mode, there may be a few other weaker modes of the system. We propose that the QBO is not a primary oscillation of the tropical coupled ocean–atmosphere system, but arises as a result of interactions between a specified LF primary ENSO mode and atmospheric high-frequency synoptic and intraseasonal disturbances that are modulated by the annual cycle (solar forcing). Although in reality, the ENSO mode is more complex, we idealize it to have a period of four years.

To model the essence of this complex interaction by a low-order model, we note that the LF ENSO mode has planetary scales (length scale of about 6000–7000 km similar to the observed ENSO anomaly scales). For such planetary-scale phenomena the nonlinear effects are not expected to be strong as the equatorial Rossby number $U/\beta_0 L^2$ (where U is a typical velocity scale, L is the length scale, and β_0 is equatorial gradient of the Coriolis parameter) is quite small. Therefore, we assume that the low-frequency oscillation may be considered as a linear oscillator. Analog models (Battisti and Hirst 1989) derived from the basic thermodynamic equation indicate that the nonlinearity may be important only in limiting the amplitude of these oscillations. On the other hand, the atmospheric synoptic oscillations have much shorter scales and, for them, the advective nonlinearity is important. Thus, the evolution of the coupled system may be represented by an interaction between a low-frequency linear oscillator and some high-frequency nonlinear waves.

To represent the nonlinear interactions between the high-frequency waves, we choose a prototype nonlinear system used by Lorenz (1984, 1990) to describe some aspects of the general circulation of the atmosphere. Coupling these nonlinear equations to a linear oscillator, the equations for the coupled system may be written as

$$\dot{X} = -Y^2 - Z^2 - aX + aF, \tag{1}$$

$$\dot{Y} = XY - bXZ - CY + G + \alpha P, \tag{2}$$

$$\dot{Z} = bXY + XZ - CZ + \alpha Q, \tag{3}$$

$$\dot{P} = -\omega Q - \beta Y, \tag{4}$$

$$\dot{Q} = \omega P - \beta Z, \tag{5}$$

where ω is the frequency of the low-frequency oscillator with a period of four years, P and Q are amplitudes of the sine and cosine phases of the oscillation, and α and β are coupling strengths. Equations (1)–(3) represent the high-frequency component, and (4)–(5) represent the low-frequency component. The typical period of oscillation of the high-frequency modes is in the synoptic range. In order that the nonlinear system (1)–(3) is flexible to represent other scales of motion such as the intraseasonal oscillations, we have rescaled Lorenz's (1984) equations by a factor C as (original variables denoted by prime)

$$t = t'/C, X = CX', Y = CY', Z = CZ',$$

$$a = a'C, b = b', F = CF', \text{and } G = C^2G'.$$

As Lorenz (1984) discusses, X may be interpreted as a zonally averaged field, while Y and Z may be interpreted as amplitudes of two wave components. The linear terms in Eqs. (1)–(3), (aX, CY, CZ) represent mechanical and thermal damping. The nonlinear terms XY and XZ represent amplification of the eddies through interaction with the mean zonal flow (X). This amplification is at the expense of the mean zonal flow indicated by the terms $-Y^2$ and $-Z^2$ in Eq. (1). The terms bXZ and bXY represent displacement of the eddies by the zonal current. The terms F and G are forcings, where F may be interpreted as external zonally symmetric forcing (e.g., solar forcing), while G is the zonally asymmetric forcing (e.g., land–ocean contrast). The annual cycle is introduced in the zonally symmetric component of the forcing, and we write $F = F_0 + F_1 \cos \pi t/\tau_1$, where τ_1 is 1 yr. Equations (1)–(3), represent the atmosphere with its annual cycle and the high-frequency oscillations, while Eqs. (4)–(5), represent the ocean primarily contain the LF oscillation. The system (1)–(5) may be considered as a "toy model" for the coupled system to derive insight regarding the nonlinear interactions in the system. In some ways, our conceptual model is similar to studies of the coupled ocean–atmosphere system (Schopf and Suarez 1988; Battisti 1988) where a linear model is forced by a white noise forcing. In our model, the white noise forcing arises from nonlinear interactions in the atmosphere.

The coupling of the high-frequency oscillations to the low-frequency oscillations is assumed to take place through the nonzonal components (Y, Z). This is based on the following qualitative arguments. For our purposes here, we assumed that the low-frequency component has a prominent wavenumber-1-type zonal pattern. Such changes in SST give rise to modulation of the atmospheric convective heating with similar east–west asymmetry. Thus, the variations associated with the low-frequency oscillation may be considered to give rise to zonally asymmetric heating in the atmosphere. This is why the coupling is added to the nonzonal component of the atmospheric component.

Thus, our toy model contains several important ingredients of the coupled air–sea interactions, namely (a) recognition of coexistence of a low-frequency-coupled mode and high-frequency modes (primarily coming from the atmosphere), (b) inclusion of appropriate nonlinearity for the high-frequency modes, (c) modulation of the climatic attractor for the high frequency by the annually varying forcing, and (d) a physically plausible coupling between the low- and the high-frequency oscillations.

In our model, the unscaled values of the coefficients a and b are $a' = 0.25$ and $b' = 4.0$. These values are the same as those used by Lorenz. The Eqs. (1)–(5) are solved numerically using a fourth-order Taylor-series scheme. Nondimensional value of the time step is $\Delta t = 0.025$, which corresponds to about three hours for the case with $C = 1.0$. Two typical time series of X for 10 years each are shown in Fig. 1, corresponding to $C = 0.5$ and $C = 1.0$, respectively, without coupling the nonlinear system with the linear oscillator ($\alpha = 0$). This figure shows the characteristic timescales represented by the low-order nonlinear system corresponding to $C = 0.5$ and $C = 1.0$, respectively. We note that $C = 1.0$ represents roughly synoptic oscillations with typical periods between 15–20 days, while $C = 0.5$ represents roughly intraseasonal oscillations with typical periods between three–four months. The nonlinear high-frequency oscillations have two preferred regimes of oscillations, one active regime (similar to the boreal summer in the Tropics) with relatively lower-frequency oscillations, and another weak regime (similar to the boreal winter in the Tropics) with relatively higher-frequency oscillations. This is somewhat similar to summer to winter flip-flop in Brier's or Nicholls' models. However, the transition here is smooth and more physical.

3. Results and discussions

Having recognized the primary existence of the LF ENSO mode, the annual cycle, and the atmospheric high-frequency oscillations, we demonstrate in this section that the tropospheric QBO may not be a primary oscillation of the coupled system, but may arise as a result of interactions between the LF ENSO mode and the atmospheric high-frequency oscillations in the presence of an annual cycle. To derive insight regarding how this happens, we present a number of sensitivity experiments with our toy model. For most of the experiments discussed below, our model is integrated for 2^{17} days or about 360 years. The data are saved once a day. Some results were tested with 540-year runs, and the power spectra presented here were found to be stable. The power spectra presented for most of the experiments described below are calculated using the Blackman and Tukey (1958) method and described in WMO (1966).

A word of explanation regarding the coupling constants α and β used in our experiments is in order here.

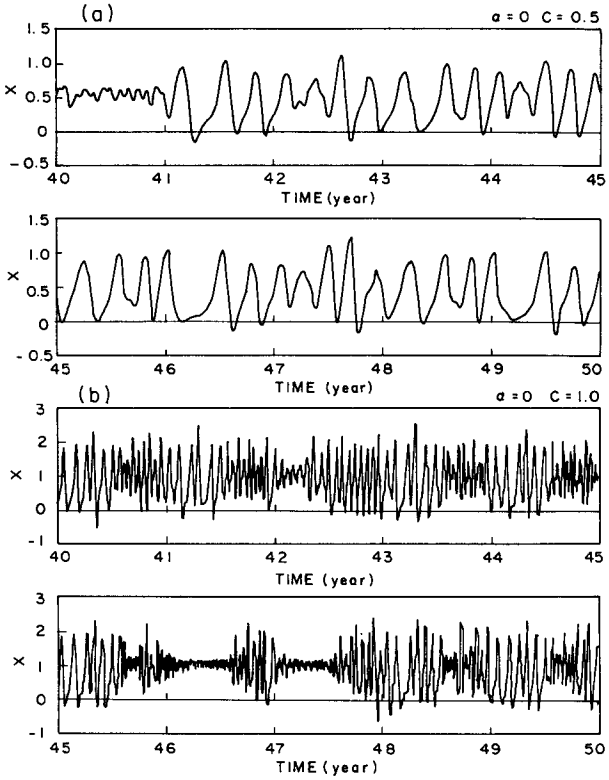

FIG. 1. The series of uncoupled ($\alpha = 0$) X for 10 yr after an initial period of 40 yr for (a) $C = 0.5$ and (b) $C = 1.0$.

As we recall, α may be interpreted as a factor relating SST to atmospheric heating, while β may be thought of as a factor relating surface wind stresses to SST. It is well known that the dependence of atmospheric convective heating on SST is a nonlinear one with a threshold (about 26.5°C) below which convection rarely occurs. Above this threshold, convection increases slowly till about 27.5°C, above which it increases dramatically with SST till about 29.5°C (Waliser et al. 1993). Thus, the coupling is strong over the warm pool region in the Indian Ocean and western Pacific, while it may be weak over colder waters in the eastern Pacific. The two values of α (0.1 and 0.125) taken in some experiments are meant to represent such strong and weak coupling conditions.

a. The base experiment

The nonlinear system (1)–(3) has a chaotic attractor for constant forcing F between 7.5 and 8.8. In order that the annual cycle contain this range of forcing, the annual cycle has been assumed as $F' = F'_0 + F'_1 \cos 2\pi t/\tau_1$ with $F'_0 = 7.0$ and $F'_1 = 2.0$. The forcing associated with the east–west heating contrast has been taken as $G' = 1.0$. In Fig. 2, we show power spectra of P (one of the LF variables) for two coupling strengths. In the absence of the coupling to the high-frequency

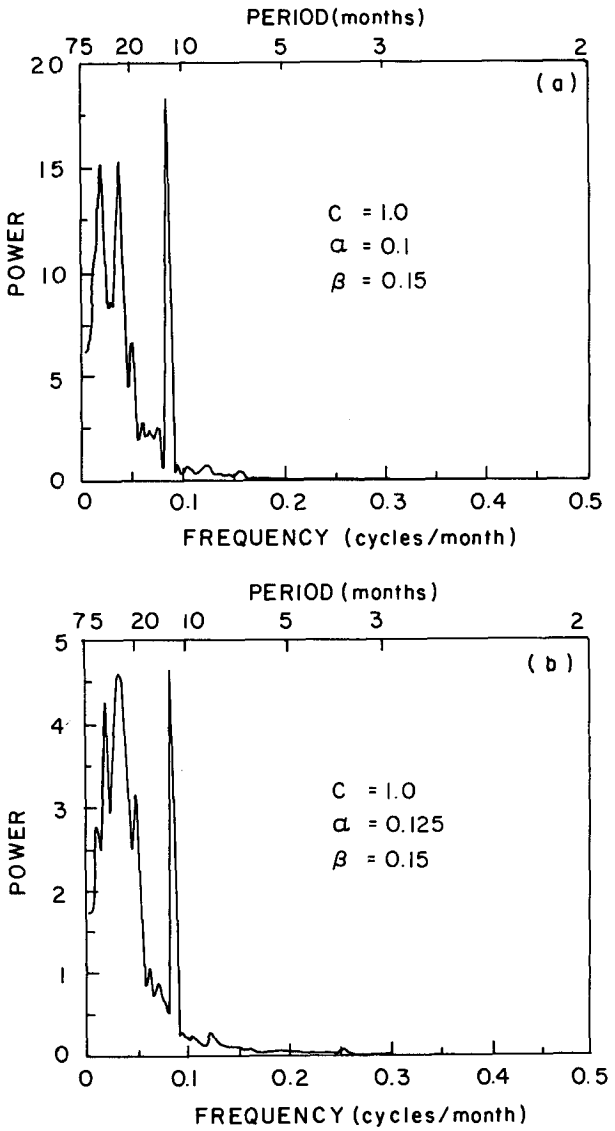

FIG. 2. Power spectrum of P for the base experiment with $C = 1.0$ and with standard annual cycle ($F_0' = 7.0$, $F_0' = 2.0$). (a) $\alpha = 0.1$ and $\beta = 0.15$, (b) $\alpha = 0.125$.

component, the LF has a pure four-year cycle. The interaction with the atmosphere broadens the LF spectrum with two clear and significant peaks, one with a period around four years and another with a period around two years. Statistical significance tests (not shown) show that the peaks with a period around four years, two years, and one year are significant at the 1% level. Depending on the coupling strength, the amplitude of the QBO could be comparable or even stronger than the LFO (Rasmusson et al. 1990; Ropelewski et al. 1992). This shows that the interaction between the LF mode and the high-frequency oscillations can indeed introduce a QBO in the coupled system. This can also be seen in the atmospheric variables. As in the real atmosphere, the raw spectrum of any variable (e.g., Y) is dominated by the annual cycle (Fig. 3a). However, if we construct monthly mean Y and remove the annual cycle from it, the spectrum brings out the QBO as the dominant peak (as is done for a Southern Oscillation index in real atmosphere). Figure 3b shows the power spectrum of monthly mean Y after removing the annual cycle. We also note from this figure that the annual signal dominates the atmospheric oscillations, with the interannual oscillations having a much smaller amplitude compared to the annual cycle (Fig. 3b), much like the real atmosphere.

The term P is a representative LF variable such as SST or a five-month running mean of surface winds. For the purpose of discussion on the origin of the QBO,

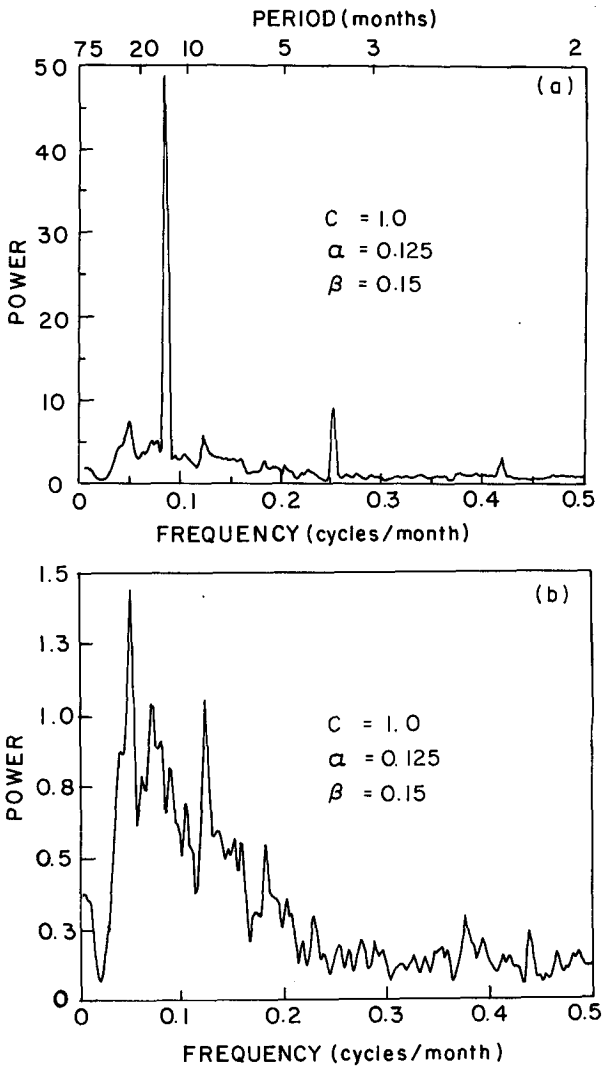

FIG. 3. Power spectrum of (a) raw Y and (b) monthly mean Y after removing the annual cycle ($C = 1.0$, $\alpha = 0.125$, and $\alpha = 0.15$) with standard annual cycle forcing as in Fig. 2.

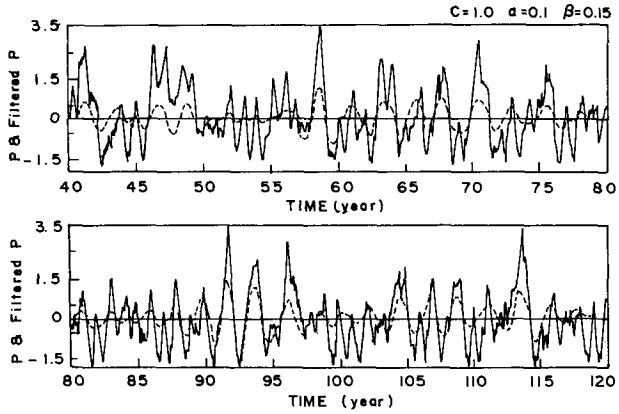

FIG. 4. Raw time series of P for 80 years (solid line) together with biennial-filtered P (dashed line) (α = 0.1, β = 0.15 and standard annual cycle C = 1.0).

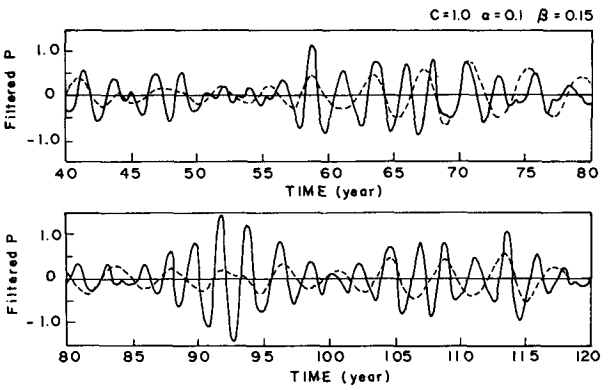

FIG. 5. Biennial-filtered P for 80 years (solid line) with LF-filtered P (dashed line) (α = 0.1, β = 0.15, and standard annual cycle C = 1.0).

it may be sufficient for us to confine ourselves primarily to this variable.

To have some idea of the relative importance of the LF oscillation and the QBO with respect to the raw time series, we examined the filtered time series for the LF oscillation as well as for the QBO. For this purpose we have used a second-order Butterworth filter similar to the one used by Murakami (1979). For the LF oscillation, the filter has peak response at a period of 50 months and half response at periods of 60 and 41.5 months, respectively. For the QBO, the filter has a peak response at a period of 25 months, while it has half response at periods of 30 and 20 months, respectively. In Fig. 4, we show the filtered QBO time series along with the raw time series of P. Similarly in Fig. 5, we show the filtered time series for the LFO and compare it with that for the QBO. These two figures contain many features of the observed QBO as discussed by Rasmusson et al. (1990) and Ropelewski et al. (1992). For example, the QBO amplitude is quite comparable to the amplitude of the LFO. Moreover, many peaks of the QBO coincide with peaks of the LFO. Also, many of the peaks of the QBO coincide with peaks of the raw time series. This illustrates that the QBO and the LFO are closely linked, as described by Barnett (1991).

b. *Role of the annual cycle*

As mentioned in the introduction, the observed QBO is strongly linked with the annual cycle. In our model too, the annual cycle plays a crucial role in producing the QBO. To illustrate this, we carried out an integration of the coupled system without an annual cycle in the forcing for the high frequency (HF) component. We fixed the forcing at the central value of the annual cycle and set F_0' = 8.0 and F_1' = 0.0. For this run, the power spectrum of P is shown in Fig. 6. Although the interaction with the HF component results in a weak broadening of the LFO around the four-year period, no response is generated around the two-year period. Similarly, no two-year period is seen in the monthly mean X spectrum (not shown). This clearly demonstrates that the annual cycle plays a crucial role in the generation of the QBO in the model-coupled system.

c. *Role of the LF oscillation*

Does the LFO play an active role or a passive role in generating the QBO? We show that the LFO indeed plays an active role in generating the QBO. It does this by modulating the forcing for the HF at the low frequency. If we insist that the coupling between the LF and HF is only one way so that the LF gets modified by the HF ($\beta \neq 0$), but the HF does not get affected

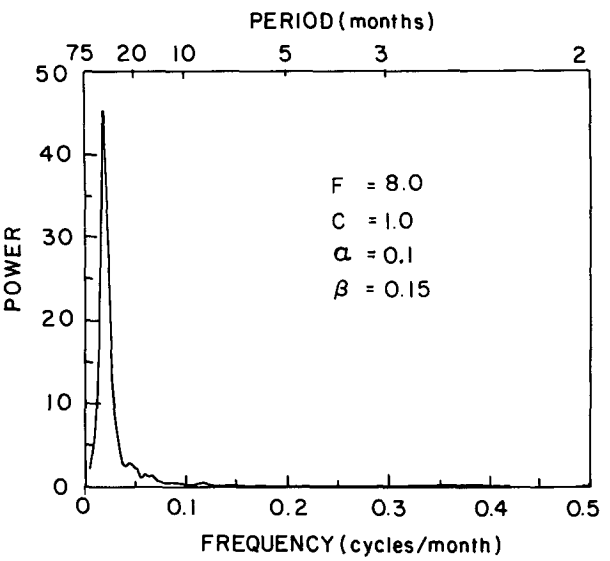

FIG. 6. Role of the annual cycle forcing. Spectrum of P for C = 1.0, α = 0.1, and β = 0.15, but for a constant forcing F_0' = 8.0 and F_1' = 0.0.

by the LF ($\alpha = 0$), then the HF cannot introduce any QBO signal in the LF component, even in the presence of an annual cycle in the HF. This is shown in Fig. 7, where the spectrum of P is shown for $\alpha = 0$ and $\beta = 0.15$ and $F_0' = 7.0$ and $F_1' = 2.0$. Thus, modulation of the forcing for the HF by the LF seems to be essential for a significant QBO response in the coupled system. The annual cycle by itself is not sufficient, and an active role by the LF in modulating the HF is necessary. This is consistent with strong interactions between the annual cycle, the QBO, and the LFO as found by Barnett (1991).

d. Role of synoptic versus intraseasonal oscillations

For all the experiments discussed so far, we have used $C = 1.0$. This corresponds to the characteristic timescale for the HF component in the synoptic range. We may ask whether the intraseasonal oscillations could do the same. To answer this question, we carried out a few experiments with $C = 0.5$. As mentioned in the previous section and shown in Fig. 1, the characteristic timescale of the HF oscillation in this case is a few months (intraseasonal range); Fig. 8 shows the power spectrum of P for $C = 0.5$, $\alpha = 0.125$, and $\beta = 0.15$, and with the standard annual cycle. It is seen that although it broadens the LF peak somewhat more than the case corresponding to $C = 1.0$, it produces only a weak biennial component. Thus, it appears that the intraseasonal oscillations are not efficient in producing a QBO in coupled variables through interaction with the LFO. However, if we examine the atmospheric variables, there is a significant QBO in the atmospheric field (Fig. 9). In Fig. 9a, we note that apart from the annual peak, the QBO with a peak around 23 months is the largest low-frequency peak. Figure 9b shows that this peak is present even if the HF component is not coupled to the LF component ($\alpha = 0$). This means that the nonlinear intraseasonal oscillations, modulated by the annual cycle, can produce a QBO in a manner similar to the one envisaged in the Brier and Nicholls models.

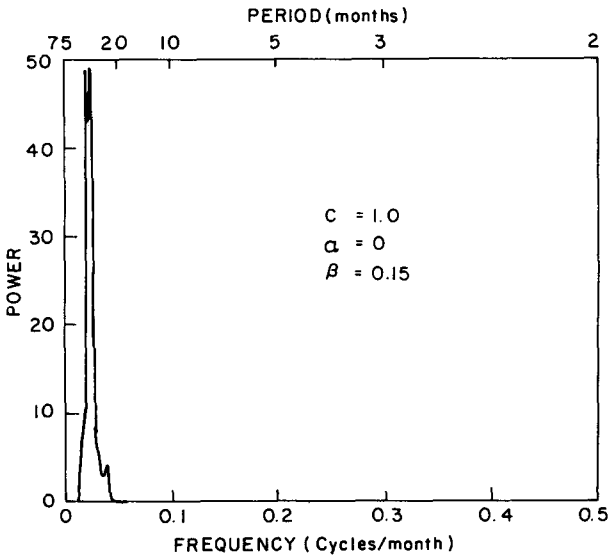

FIG. 7. Role of the LF modulation of the forcing for the atmospheric oscillations. Spectrum of P for $C = 1.0$, $\alpha = 0.0$, $\beta = 0.15$, and standard annual cycle.

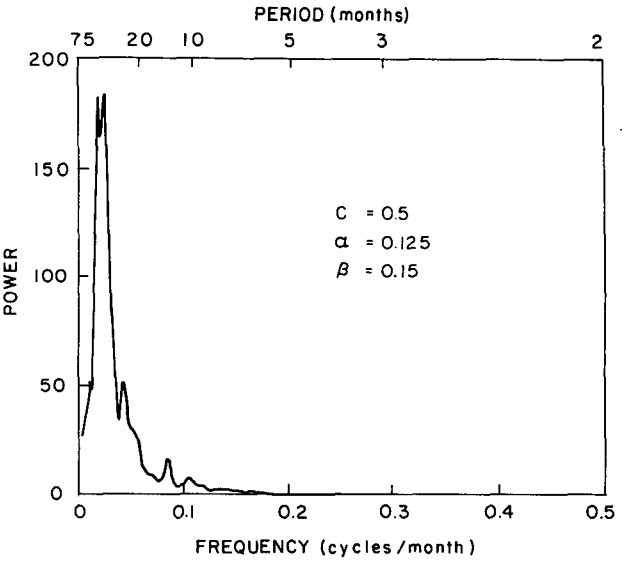

FIG. 8. Spectrum of P for $C = 0.5$, $\alpha = 0.125$, and $\beta = 0.15$ with standard annual cycle.

In Fig. 10, we show the raw spectrum of Y in the absence of either an annual cycle or an LF oscillation for $C = 1.0$ and $C = 0.5$, respectively. It is noted that the nonlinear interactions between the synoptic scales or between the interseasonal waves themselves cannot produce any significant LF response. If the dominant atmospheric nonlinear oscillations are in the interseasonal range, the annual cycle itself can generate a significant QBO in the atmosphere (Fig. 9). On the other hand, if the dominant atmospheric nonlinear oscillations are in the synoptic range, a significant QBO could be obtained only if they have an annual forcing and are coupled to an LF oscillation (see Fig. 6 and discussions on the previous subsection.) This and the results presented in the previous paragraph (Fig. 9) may explain some observations as noted by Rasmusson et al. (1990) and Ropelewski et al. (1992). They note that the QBO in the SST field has the largest amplitude in the eastern Pacific, while that in the zonal wind has largest amplitude in the eastern Indian Ocean and western Pacific (i.e., the warm pool). We recall that the warm pool is also the region of the largest intraseasonal oscillations (ISO). Therefore, in the warm pool region, the strong ISO in the atmosphere, interacting with the annual cycle, produces a strong QBO in the atmosphere and the coupling produces a weak QBO in the ocean. On the other hand, in the eastern

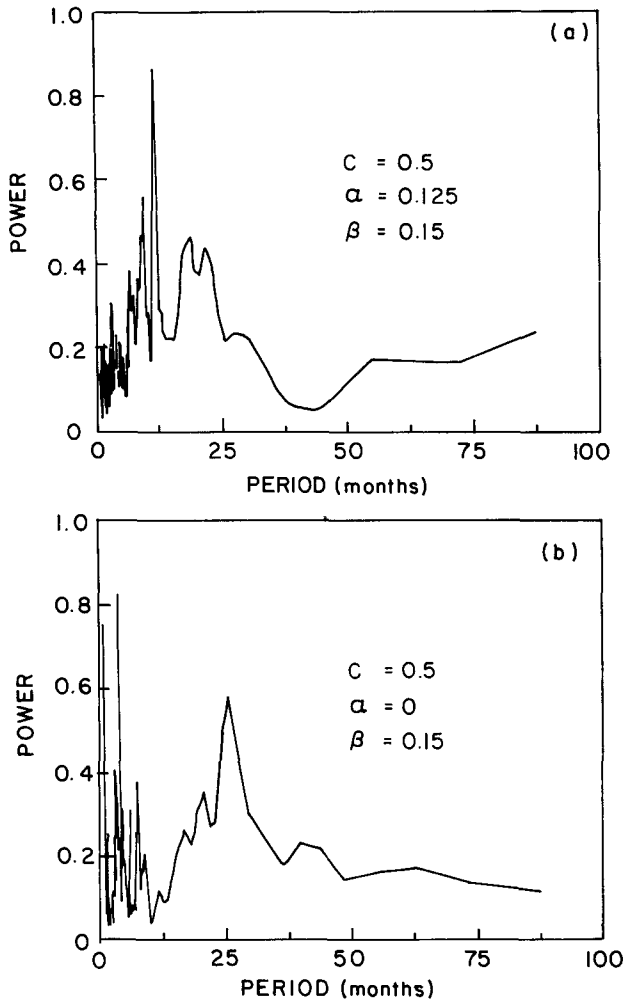

FIG. 9. Spectrum of Y for (a) $C = 0.5$, $\alpha = 0.125$, $\beta = 0.15$ and (b) $C = 0.5$, $\alpha = 0.0$, and $\beta = 0.15$. Both have standard annual cycle.

Pacific, there is hardly any ISO, and, hence, coupling between the atmosphere and the ocean takes place mainly through synoptic activity. This produces a weak QBO in the atmosphere and a strong QBO in the ocean.

4. Conclusions

We propose that the tropospheric QBO is neither a tropospheric manifestation of the stratospheric QBO, nor is it a fundamental mode of oscillation of the tropical coupled system. It is possible that it may arise due to multiscale interaction between nonlinear synoptic and intraseasonal atmospheric oscillations and a specified LF coupled mode in the presence of the annual cycle. We demonstrate this using a conceptual model of the coupled system. Our conceptual model consists of a low-order system representing the nonlinear atmospheric HF and intraseasonal oscillations modulated by an annual cycle forcing, which is coupled to a linear oscillator with a four-year period representing the coupled LF mode. The LF mode is considered as a linear oscillator as the horizontal scale of this mode is very large (6000–7000 km), and, hence, the advective nonlinearities associated with this mode are weak. Some important observed characteristics of the QBO, such as the importance of the annual cycle and interaction with the ENSO cycle, are contained in the model. Both the synoptic and the intraseasonal oscillations of the atmosphere may take part in the interaction. If the intraseasonal oscillations are dominating, the QBO in the atmosphere may be strong, while the one in the ocean may be weak. On the other hand, if the synoptic disturbances are dominating, the QBO in the ocean is expected to be strong, while the one in the atmosphere is expected to be weak. This seems to agree well with the observation that the QBO in SST is strong and that in zonal wind is weak in the eastern Pacific, while the reverse is true in the eastern Indian Ocean

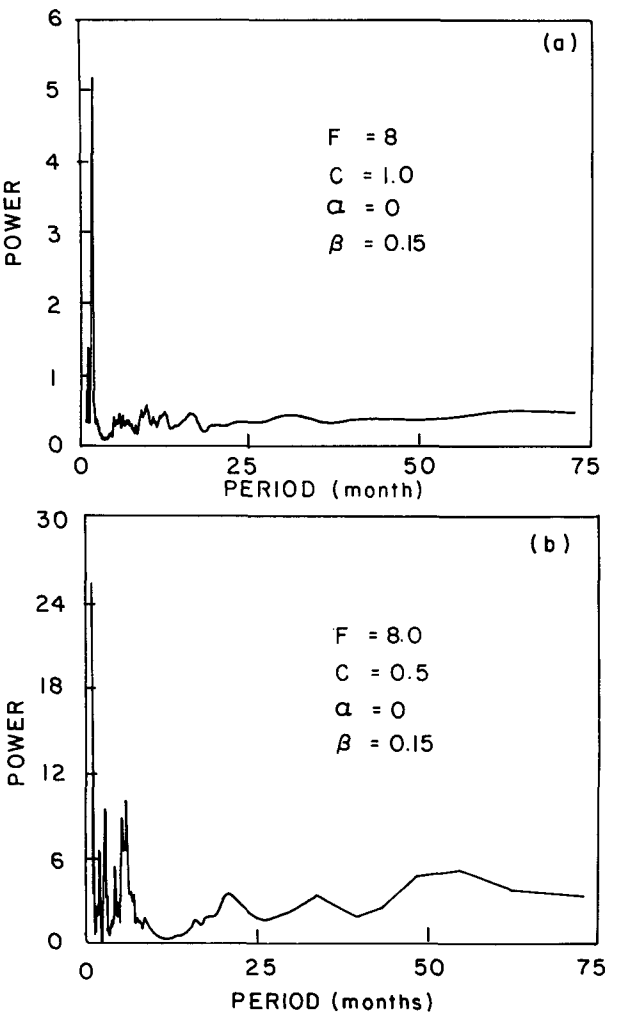

FIG. 10. Uncoupled spectrum of Y ($\alpha = 0$) with constant forcing $F = 8.0$. (a) $C = 1.0$, (b) $C = 0.5$.

and western Pacific where intraseasonal oscillations are the strongest. It is shown that in the absence of the annual cycle, QBO cannot be generated either in the atmospheric fields or in the oceanic fields. Even with the annual cycle, coupling of the HF to the LF oscillations is essential to generate the QBO in the ocean.

The spectrum of interannual variability in the Tropics (Rasmusson and Carpenter 1982) shows that the ENSO mode with a period of about four years is the dominant mode of oscillation. However, it is not a line spectrum but it has a band of period around the dominant periodicity. This broadband nature of the ENSO makes it aperiodic and puts a limit on the predictability of the system. Our simple model shows that the basic four-year oscillation, generated by the coupled instability and wave dynamics, is modified through interactions with the nonlinear HF atmospheric component so that its spectrum is broadened (Fig. 2). Thus, not only the QBO is generated through the interaction between the LFO and the HF oscillations, the aperiodicity in the LFO is also introduced through the same interactions. A detailed discussion on how the aperiodicity of the ENSO could be generated is provided elsewhere (Krishnamurthy et al. 1993).

Some insight as to how the coupling between the LF and the HF nonlinear oscillations work may be obtained from the following considerations. In the absence of the coupling, the LF is assumed to be a pure linear oscillation with a period of four years. In the absence of coupling ($\alpha = 0$), the nonlinear system, however, has a broad band of high frequencies but no appreciable signal in the low frequencies (Fig. 10). To the zeroeth order, we can imagine the coupling to the nonlinear system as a time-dependent forcing for the LF system. Since, the LF system is a [Eqs. (5)–(6)] linear-forced system, it can have appreciable response only near the resonance around the four-year period. If the nonlinear system does not have appreciable power around this period (as in the case without annual cycle, $C = 1.0$, $F = 8.0$, Fig. 10a), the coupling to the nonlinear system does not modify the linear oscillator (as in Fig. 6). Therefore, to produce the broadening of the four year spectrum (i.e., aperiodicity in the LF component) as well as a QB response in the coupled variables (or the oceanic variables), the atmospheric component must be capable of producing a low-frequency tail in their spectrum.

How does the atmosphere generate a low-frequency response? It does it through modulation of its forcing by the annual cycle or by the LF through coupling. How does periodic variation of forcing for the atmosphere with a period of 1 yr or 4 yr generate responses at all low frequencies? This was discussed by Lorenz (1990) in detail. To understand how the slowly varying forcing introduces the low-frequency response, we need to examine the nature of variations of the nonlinear system (1)–(3) for different values of the steady forcing ($F_1 = 0$). In Fig. 11a, we show some gross characteristics of the attractors (long-term mean and standard deviation) of the system (1)–(3) for a range of values of F. The two symbols represent attractors attained from two different initial conditions. The system has periodic attractors for F between 5.0 and 7.5. For F between 7.5 and 8.8, the system has a chaotic attractor. Beyond $F = 8.8$, again the system goes to a periodic regime. We note that for F between 5.0 and 7.0, the system has at least two periodic orbits, one with high amplitude and low mean, while the other with low amplitude and higher mean. Within the chaotic regime too, the system tends to have two preferred regimes,

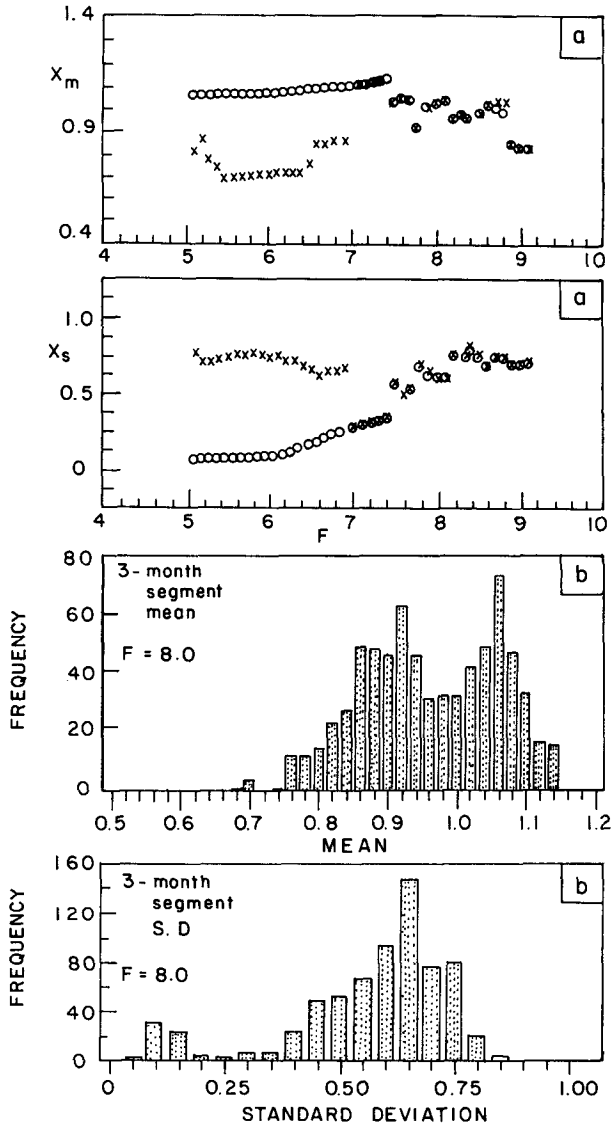

FIG. 11. Some gross features of the attractors for $\alpha = \beta = 0$ and $C = 1.0$ with no annual cycle in F and constant G ($G' = 1.0$, $F_1' = 0.0$). (a) Variation of long-term mean (X_m), and standard deviation (X_s) for a range of values of F. (b) Frequency distribution of mean and standard deviation for three-month segments for $F = 8.0$ over a period of 184 years.

one with large amplitude oscillations (active regime) and another with small amplitude oscillations (weak regime). This is seen in Fig. 11b where the frequency distribution of mean and standard deviation calculated over three month segments over a period of 184 yr is shown. The standard deviation shows the tendency for two preferred locations.

With this background, we may try to understand the response of the nonlinear system when the forcing changes periodically. When the forcing varies annually between two extremes, say between $F = 9$ and $F = 5$, the system reaches a chaotic attractor that consists of a strong and a weak regime. The two regimes resemble the orbits of the multiple periodic attractors of constant forcings discussed earlier. Whether the system would tend to visit the weak or the strong regime depends on the previous history of states (or initial conditions, in a loose manner) that may favor one or the other regime. At many of these values of F, when they are held constant, the system may possess multiple periodic attractors that depend on the initial conditions. But when the forcing is varying because of chaos, the system reaches a different state on the same day (or same value of T) of every year. This difference determines the difference in the subsequent behavior of the system–whether to visit the strong or the weak regime. This essentially is why the annual cycle itself is capable of introducing some interannual variability. Thus, the mechanism of generation of low-frequency signals in the nonlinear system in our model is similar to the one discussed by Lorenz (1990).

The coupling of the atmosphere to the LFO may also be considered as a slowly varying forcing for the atmosphere. The only difference with the annual cycle is that this slowly varying forcing, apart from having a lower frequency, acts on the zonally asymmetric component. This may be thought of as equivalent to slowly varying the land–ocean contrast (G). Due to the intransitivity of the nonlinear atmospheric oscillations, such a slow variation in G also produces a broad low-frequency response in the atmosphere. The physical mechanism for generation of such low-frequency response is exactly similar to the one described above for the annual variation of the forcing.

Finally, we note that the major contribution of our work is to illustrate the role of the MJO-type intraseasonal oscillations in generating the QBO through interaction with the seasonal cycle and the LFO. As noted earlier, both the Meehl mechanism, as well as, to a lesser extent, the Brier and Nicholls mechanisms, involve strong ocean–atmosphere coupling at one time of the year to "set" the system for the next year of the opposite sign. The physical processes involved in this modulation of the seasonal cycle were not clearly envisaged in these studies. Recognizing the fact that the MJO modulates the seasonal convective activity, we have involved the intraseasonal oscillations explicitly in the interactions. Thus, the mechanism proposed here is built upon some basic ideas provided in earlier studies of Brier, Nicholls, and Meehl but provides further insight into how the annual cycle may help produce the QBO. Moreover, the results of Barnett (1991) are consistent with the proposed mechanism, as the nonlinear interactions of the annual cycle with itself are not essential for producing the QBO in our mechanism. In this manner, our study also helps tie up these previous studies.

Thus, an external forcing with a quasi-biennial period or an association with the stratospheric QBO may not be necessary to explain the observed tropospheric QBO. Generation of low-frequency response due to the annual cycle and its amplification by the coupling to the LF oscillation (or the ocean) could explain the observed tropospheric QBO signal. We would, however, like to add here that these results from our simple conceptual model are only suggestive of the physical processes at work in the observed system. These results need to be verified with more complex GCMs and with observations.

Acknowledgments. The author wishes to thank the Department of Science and Technology, Government of India for a grant. The author is grateful to Dr. V. Krishnamurthy for introducing him to the Lorenz's model, and Mrs. R. Rama for preparing the manuscript. He also thanks H. Annamalai for help in some computations. The author is also grateful to two anonymous reviewers for some constructive comments on an earlier version of the manuscript.

REFERENCES

Anderson, D. L. T., and J. P. McCreary, 1985: Slowly propagating disturbances in a coupled ocean–atmosphere model. *J. Atmos. Sci.*, **42**, 615–629.

Barnett, T. P., 1983: Interaction of the monsoon and Pacific trade wind system at interannual time scales. Part I: The equatorial zone. *Mon. Wea. Rev.*, **111**, 756–773.

——, 1991: The interaction of multiple time scales in the tropical climate system. *J. Climate*, **4**, 269–285.

Battisti, D. S., 1988: Dynamics and thermodynamics of a warming event in a coupled tropical atmosphere–ocean model. *J. Atmos. Sci.*, **45**, 2889–2919.

——, and A. C. Hirst, 1989: Interannual variability in the tropical atmosphere–ocean system: Influence of the basic state and ocean geometry. *J. Atmos. Sci.*, **46**, 1687–1712.

Berlage, H. P., 1955: The Southern Oscillation, a 2–3 year fundamental oscillation of world wide significance. *Proc. Int. Assoc. Meteorology*, London, U.K., IUGG, 152 pp.

Bjerknes, J., 1969: Atmospheric teleconnections from the equatorial Pacific. *Mon. Wea. Rev.*, **97**, 163–172.

Blackman, R. B., and J. W. Tukey, 1958: *The Measurement of Power Spectra.* Dover, 190 pp.

Brier, G. W., 1978: The quasi-biennial oscillation and feedback processes in the atmosphere-ocean-earth system. *Mon. Wea. Rev.*, **106**, 938–946.

Cane, M. A., and S. E. Zebiak, 1985: A theory of El Nino and Southern Oscillation. *Science*, **228**, 1085–1087.

Deser, C., and J. M. Wallace, 1987: El Nino events and their relation to the Southern Oscillation: 1925–86. *J. Geophys. Res.*, **92**, 14 189–14 196.

Diaz, H. F., and R. S. Pulwarty, 1992: Comparison of Southern Oscillation and El Nino signals in the Tropics. *El Nino: Historical*

and Paleoclimatic Aspects of Southern Oscillation, H. E. Diaz and V. Markgraf, Eds., Cambridge University Press, 175–192.

Goswami, B. N., and S. Selvarajan, 1991: Convergence feedback and unstable low frequency oscillations in a simple coupled ocean-atmosphere model. *Geophys. Res. Lett.,* **18,** 991–994.

Hirst, A. C., 1986: Unstable and damped equatorial modes in simple coupled ocean–atmosphere models. *J. Atmos. Sci.,* **43,** 606–630.

Krishnamurthy, V., B. N. Goswami, and R. Legnani, 1993: A conceptual model for the aperiodicity of interannual variability in the Tropics. *Geophys. Res. Lett.,* **20,** 435–438.

Landsberg, H. E., J. M. Mitchell Jr., H. L. Crutcher, and F. T. Quinlan, 1963: Surface signs of biennial atmospheric pulse. *Mon. Wea. Rev.,* **101,** 549–556.

Latif, M., A. Sterl, E. Maier-Reimer, and M. M. Junge, 1993: Climate variability in a coupled GCM. Part I: The tropical Pacific. *J. Climate,* **6,** 5–21.

Lau, N. C., S. G. H. Philander, and M. J. Nath, 1992: Simulation of ENSO-like phenomena with a low resolution coupled GCM of the global ocean and atmosphere. *J. Climate,* **5,** 284–307.

Lorenz, E. N., 1984: Irregularity, a fundamental property of the atmosphere. *Tellus,* **A36,** 98–110.

——, 1990: Can chaos and intransitivity lead to interannual variability? *Tellus,* **A42,** 378–389.

Meehl, G. A., 1987: The annual cycle and interannual variability in the tropical Pacific and Indian Ocean region. *Mon. Wea. Rev.,* **115,** 27–50.

——, 1990: Seasonal cycle forcing of El Niño–Southern Oscillation in a global, coupled ocean–atmosphere GCM. *J. Climate,* **3,** 72–98.

——, 1993: A coupled air–sea biennial mechanism in the tropical Indian and Pacific regions: Role of the ocean. *J. Climate,* **6,** 31–41.

Murakami, M., 1979: Large-scale aspects of deep convective activity over the GATE area. *Mon. Wea. Rev.,* **107,** 994–1013.

Nagai, T., T. Takioka, M. Endoh, and Y. Kitamura, 1992: El Niño–Southern Oscillation Simulated in an MRI atmosphere–ocean coupled general circulation model. *J. Climate,* **5,** 1202–1233.

Neelin, J. G., 1991: The slow surface temperature mode and the fast wave limit: Analytic theory for tropical interannual oscillations and experiments in a hybrid coupled model. *J. Atmos. Sci.,* **48,** 584–606.

Nicholls, N., 1978: Air-sea interactions and the quasi-biennial oscillation. *Mon. Wea. Rev.,* **106,** 1505–1508.

Philander, S. G. H., T. Yamagata, and R. C. Pacanowski, 1984: Unstable air–sea interactions in the Tropics. *J. Atmos. Sci.,* **41,** 604–613.

——, R. C. Pacanowski, N. C. Lau, and M. J. Nath, 1992: Simulation of ENSO with a global atmospheric GCM coupled to a high resolution tropical Pacific Ocean GCM. *J. Climate,* **5,** 308–329.

Qiunn, W. H., 1992: A study of Southern Oscillation related activity for A. D. 622—1990 incorporating Nile River flood data. *El Nino: Historical and Paleoclimatic Aspects of Southern Oscillation,* H. F. Diaz and V. Markgraf, Eds., Cambridge University Press, 119–150.

Rasmusson, E. M., and T. H. Carpenter, 1982: Variation in tropical sea surface temperature and surface wind fields associated with Southern Oscillation/El Niño. *Mon. Wea. Rev.,* **110,** 354–384.

——, P. A. Arkin, W. Y. Chen, and J. B. Jalickee, 1981: Biennial variation in surface temperature over the United States as revealed by singular decomposition. *Mon. Wea. Rev.,* **109,** 181–192.

——, X. Wang, and C. F. Ropelewski, 1990: The biennial component of ENSO variability. *J. Mar. Sci.,* **1,** 71–96.

Ropelewski, C. F., and M. S. Halpert, 1987a: Global and regional scale precipitation patterns associated with the El Niño/Southern Oscillation. *Mon. Wea. Rev.,* **115,** 1606–1626.

——, and ——, 1987b: Precipitation patterns associated with the high index phase of the Southern Oscillation. *J. Climate,* **2,** 268–284.

——, ——, and X. Wang, 1992: Observed tropospheric biennial variability and its relationship to the Southern Oscillation. *J. Climate,* **5,** 594–614.

Schopf, P. S., and M. J. Suarez, 1988: Vascillations in a coupled ocean–atmosphere model. *J. Atmos. Sci.,* **45,** 549–566.

Sperber, K. R., and S. Hameed, 1991: Southern Oscillation in the OSU coupled upper ocean-atmosphere GCM. *Climate Dyn.,* **6,** 83–97.

Suarez, M. J., and P. S. Schopf, 1988: A delayed oscillator for ENSO. *J. Atmos. Sci.,* **46,** 3283–3287.

Trenberth, K. E., 1975: A quasi-biennial standing wave in the Southern Hemisphere and interrelations with sea surface temperature. *Quart. J. Roy. Meteor. Soc.,* **101,** 55–74.

——, 1976: Spatial and temporal variations of Southern Oscillation. *Quart. J. Roy. Meteor. Soc.,* **102,** 639–654.

——, 1980: Atmospheric quasi-biennial oscillations. *Mon. Wea. Rev.,* **108,** 1370–1377.

——, and W. T. Shin, 1984: Quasi-biennial fluctuations in sea level pressure over the Northern Hemisphere. *Mon. Wea. Rev.,* **112,** 761–777.

van Loon, H., and D. J. Shea, 1985: The Southern Oscillation. Part IV: The precursors south of 15°S to the extreems of the oscillation. *Mon. Wea. Rev.,* **113,** 2063–2974.

Wakata, Y., and E. S. Sarachik, 1991: Unstable coupled atmosphere–ocean basin modes in the presence of spatially varying basic state. *J. Atmos. Sci.,* **48,** 2060–2077.

Waliser, D., N. E. Graham, and C. Gautier, 1993: Comparison of highly reflective cloud and outgoing longwave radiation datasets for use in estimating tropical deep convection. *J. Climate,* **6,** 331–353.

WMO, 1966: Some methods in climatological analysis, WMO Tech. Note No. 81. WMO No. 199, Geneva, 53 pp.

Yamagata, T., and Y. Masumoto, 1989: A simple ocean-atmosphere coupled model for the origin of a warm El Nino Southern Oscillation. *Philos. Trans. Roy. Soc. London,* **A329,** 225–236.

Yasunari, T., 1989: A possible link of the QBO's between the stratosphere, troposphere and the surface temperature in the Tropics. *J. Meteor. Soc. Japan,* **67,** 483–493.

Zebiak, S. E., and M. A. Cane, 1987: A model El Niño–Southern Oscillation. *Mon. Wea. Rev.,* **115,** 2262–2273.